Medical & Biological Engineering & Computing (2023) 61:421–434
https://doi.org/10.1007/s11517-022-02704-y

ORIGINAL ARTICLE

The effect of the 2-UPS/RR ankle rehabilitation robot with coupling biomechanical model on muscle behaviors

You Shengxian[1] · Lu Zongxing[1] · Wang Jing[1] · Guo Lin[1]

Received: 27 June 2021 / Accepted: 21 September 2022 / Published online: 2 December 2022
© International Federation for Medical and Biological Engineering 2022

Abstract
With the popularization of biomechanical simulation technology, aiming at the rehabilitation of ankle joint injury, we imported simplified model of proposed 2-UPS/RR (two identical unconstraint kinematic branches with a universal–prismatic–spherical (UPS) structure and two rotating pair (R)) ankle rehabilitation robot into AnyBody Modeling System. Therefore, a human–machine model was established using the HILL-type muscle model and muscle recruitment criteria. This paper investigated the effects of rehabilitation trajectories on biomechanical response during rehabilitation. Additionally, three main lower limb muscles (soleus, peroneal brevis, and extensor digitorum longus) were examined under different rehabilitation trajectories (plantar dorsiflexion, varus or valgus, and compound movement) in the present study. Based on the biomechanical response of lower limbs, the results showed that different muscles had different sensitivities to the change of rehabilitation trajectories. The correlation coefficient between joint force and plantar dorsiflexion angle reached 0.99 ($P < 0.01$), indicating that the change of joint force was mainly dominated by plantar dorsiflexion/plantar flexion, but also affected by varus or valgus. Safe rehabilitation training can be achieved by controlling the designed 2-UPS/RR rehabilitation robot. The behavior of muscle force and joint force under different rehabilitation trajectories can meet the needs of rehabilitation and treatment of joint diseases, and provide more reasonable suggestions for early rehabilitation.

Keywords Biomechanical simulation · Human–machine coupling model · Lower limb rehabilitation · Ankle · Rehabilitation robot

1 Introduction

Biomechanics simulation refers to realize virtual analysis and simulation research on the mechanics principles of living organisms by applying mechanics principles and methods and combining virtual reality technology. Using virtual simulation technology can not only improve the realism of moving objects, but also save research and development (R&D) costs and improve R&D efficiency, reducing the difficulty o0f data analysis significantly. Therefore, this technology is now widely used in various fields of medical rehabilitation.

In current research, biomechanical simulation has been widely used in various fields [1]. Van Houcke J et al. [1] evaluated the hip joint reaction force and hip flexion angle in a virtual representative male Caucasian population by means of musculoskeletal modeling of three distinct sitting configurations; they showed that the different sitting configurations can affect the hip joint. Elham Hazrati [2] studied the biomechanical response of lower limbs (muscle activation and joint force) through pedal man–machine model; they investigated that the saddle place can affect the muscles and joints behavior. Apoorva Rajagopal et al. [3] established a gait man–machine model based on the HILL-type model, tested the model by simulating the accuracy of healthy walking and running, and generated an accurate gait simulation. Samuel R. Hamner et al. [4] developed a three-dimensional muscle drive model of the running gait cycle. Through an analysis of the model, the different contribution degree of each muscle in resting state and exercise state was determined. Lu Zongxing et al. [5] established a human–machine coupling model of disuse atrophy of lower extremity muscles and determined the different contributions of each muscle in the resting state and in moving state

✉ Lu Zongxing
luzongxing@fzu.edu.cn

[1] School of Mechanical Engineering and Automation, Fuzhou University, No. 2 Xueyuan Road, Fuzhou 350116, Fujian, China

by analyzing model. Some previous studies have combined biomechanics with ankle rehabilitation robots; Zeng fenfang et al. [6] created a computational biomechanical model of the human ankle for the rehabilitation robot, and put this theoretical model on the ankle rehabilitation robot. Min shi et al. [7] proposed a man–machine collaboration model of an EEG-driven ankle joint rehabilitation robot. The above two articles mainly focus on the establishment of related biomechanical models, and lack of research on specific parameters of ankle joint rehabilitation robot.

As one of the most complex joints in the human body, the ankle joint plays an important role in daily life and is also vulnerable to get injured. During the course of traditional physiotherapy, the patient's ankle is manually moved by therapist. A series of ankle rehabilitation robot has been invented. In the past, many studies have conducted in-depth discussions on how to solve the scope of robot rehabilitation and the configuration of the mechanism. Yongfeng Wang [8] designed a new type of parallel ankle joint rehabilitation robot which realized kinematics solution and simulation analysis. According to three inputs condition, it was properly to meet the range of motion for the normal ankle. Dai [9] proposed a 3-SPS/SP (three spherical–prismatic–spherical kinematic branch) parallel tripod-type mechanisms for sprained ankle treatment based on the study of ankle functional anatomy. Jamwal [10] proposed a flexible parallel rehabilitation robot for ankle joint rehabilitation; they proposed a modified fuzzy inference system to solve the forward kinematics to optimize parameters. Saglia et al. [11] put forth a 3-UPS/U redundantly actuated parallel mechanism with the advantage of mechanical and kinematical simplicity to produce the 2-DOF plantarflexion/dorsiflexion and inversion/eversion assistive and resistive rehabilitations.

At present, the research on ankle rehabilitation robots mostly stays in institutional research and optimization and the importance of rehabilitation trajectory in formulating rehabilitation robot strategies. It is necessary to reveal the changes in rehabilitation trajectory and lower extremity muscle behavior. To investigate the influence of the effective factors on the body, we can use simulation methods. The simulation methods can avoid the statistical population, where the conditions of the subjects influence the study. However, in the simulation, the model as a representative of the complex body system allows to change only one parameter in the absence of the noise from other changing parameters. Also, the model can investigate the relationship between rehabilitation trajectory and muscle behavior without the fatigue.

To date, ergonomic studies of ankle rehabilitation robot have mainly focus on structure and sports space. Up until now, the lower limb biomechanics has not been the subject of such analysis. Therefore, the aim of the article was to provide initial insight into biological changes in lower limbs and rehabilitation trajectory that are relevant to daily exercise rehabilitation. Firstly, we established a coupling model of human body and ankle rehabilitation robot using a biomechanical analysis software. Secondly, we conducted a surface EMG verification test to verify the accuracy of the established human–machine coupling model. Thirdly, we investigated the changing trend of lower limb muscle strength under different rehabilitation trajectories. In addition, it provides insight into the biomechanical variables that are difficult or impossible to measure directly (such as muscles force or joints reaction force).

2 Methods

2.1 Establish a man–machine coupling model

To lower extremity biomechanical ankle rehabilitation response characteristics, this paper proposed a 2-UPS/RR ankle joint rehabilitation robot as the research object, coupling the display unit to carry out simulation analyses of biomechanical rehabilitation process characterized in that among the lower extremities. After the coupling model was established, a real machine experiment was performed on healthy people to collect biomechanical data of the lower limbs to verify the accuracy of the established model.

This study uses the AnyBody Modeling System (AMS) for man–machine coupling simulation under different rehabilitation trajectories. AMS provided a complete body system of bones, muscles, and ligaments. When establishing the human–machine coupling model, the upper limbs are ignored and most of the upper limb muscles are removed so that there is a faster calculation rate when establishing the model. The model has 84 muscles in the lower limbs. In addition, the hip, knee, and ankle joints of this model have three, one, and two degrees of freedom, respectively. The analysis flow chart is shown in Fig. 1.

AnyBody's built-in Fourier driver is used to drive the 2-UPS/RR ankle rehabilitation robot. The nutation motion trajectory of the ankle joint rehabilitation robot is mainly analyzed; the movement of the movable platform is mainly composed of the combination of plantar dorsiflexion and varus, and the driving function of the motion trajectory of plantar dorsiflexion and varus is as follows:

$$a = \sum_{i=1}^{2} A_i \cos\left(w_i t + B_i\right) \tag{1}$$

$$\beta = \sum_{k=1}^{2} A_k \ \sin(w_k t + B_k) \tag{2}$$

Among them:

$$w_i = (i-1)2\pi f \quad w_k = (k-1)2\pi f \tag{3}$$

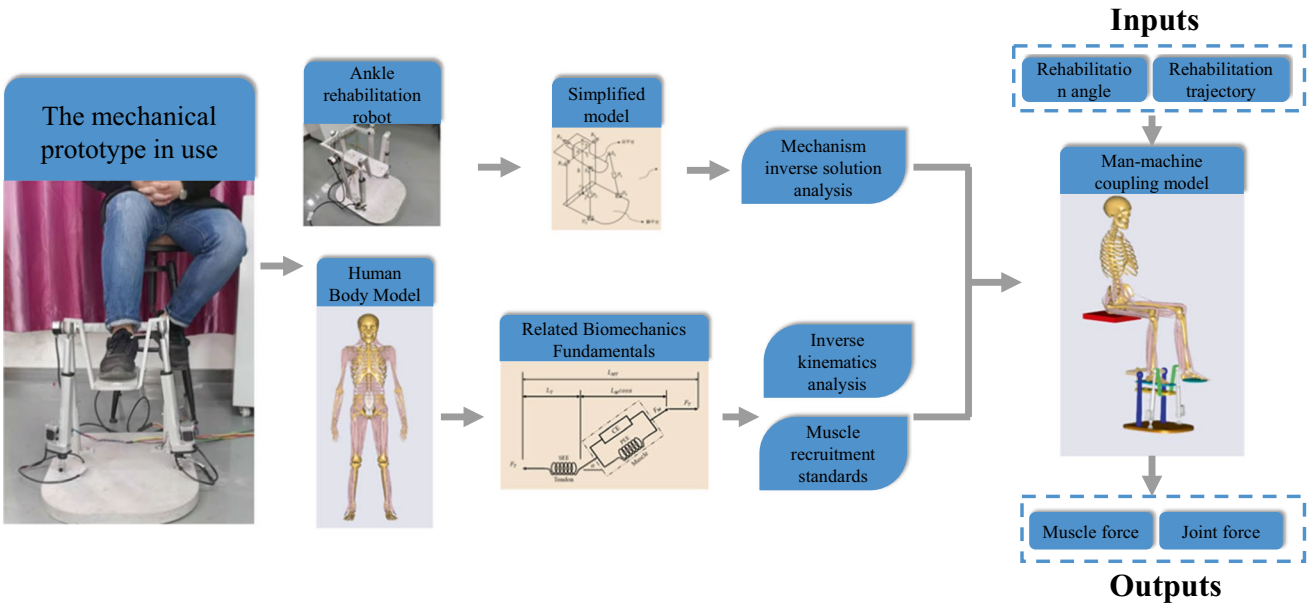

Fig. 1 Man–machine coupling model analysis process

$$A_i=[A_1,A_2]\ \ B_i=[B_1,B_2] \tag{4}$$

where α and β are the dorsiflexion plantar and varus driver functions, A_i and B_i are the Fourier coefficients, and f is the frequency.

2.2 Mechanism inverse solution analysis

The static platform is connected with the branch chain through the universal pair at U_1 and U_2 and the fixed end at O. The moving platform is connected with the branch chain through the ball pair at S_1 and S_2. The extension lines of R_1 and R_2 intersect at point O'; moreover, O' is the virtual center point of the ankle joint in rehabilitation exercises. There is a moving pair on branch 1 and branch 2. A dynamic coordinate system O'-uvw was established at A_3, and a static coordinate system $O-xyz$ was established at B_3 (Fig. 2).

According to the closed-loop vector method, the equation is obtained:

$$l_i=-u_i+h+s_i,\ i=1,2 \tag{5}$$

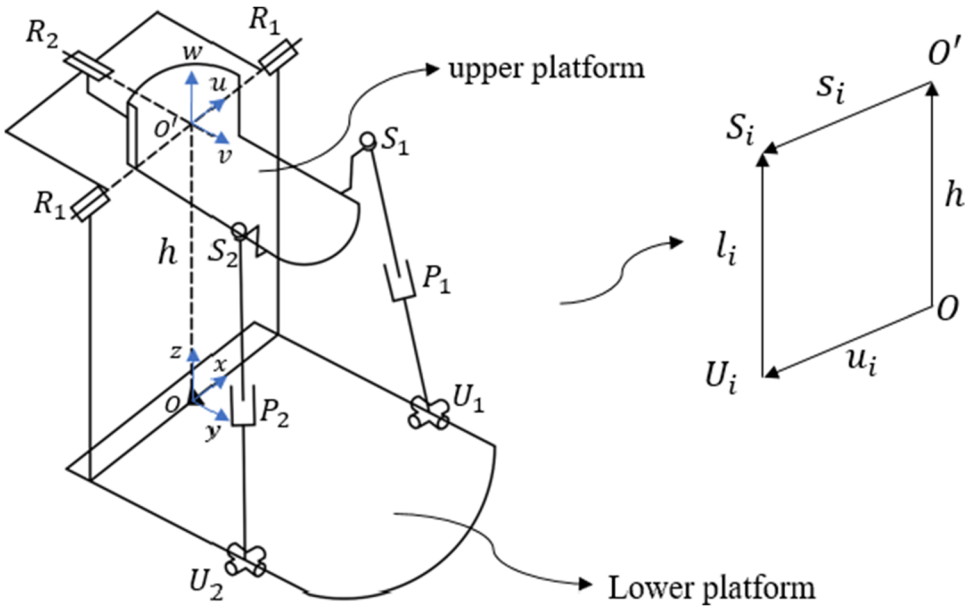

Fig. 2 A2-UPS/RR organization diagram

l_i is the length of each link, u_i represents the position vector from O to U_i, s_i represents the position vector from O' to S_i, α and β are used to indicate the angle that the mechanism has rotated around the x and y axis, and h represents the distance from O to the ankle compound center. The rotation matrices are:

$$R(x,\alpha)=\begin{bmatrix}1 & 0 & 0\\ 0 & c\alpha & -s\alpha\\ 0 & s\alpha & c\alpha\end{bmatrix} \tag{6}$$

$$R(y,\beta)=\begin{bmatrix}c\beta & 0 & s\beta\\ 0 & 0 & 1\\ -s\beta & 0 & c\beta\end{bmatrix} \tag{7}$$

The rotation matrix of the dynamic coordinate system relative to the static coordinate system can be obtained as:

$$R=R(x,\alpha)R(y,\beta)=\begin{bmatrix}c\beta & 0 & s\beta\\ s\alpha s\beta & c\alpha & -s\alpha c\beta\\ -c\alpha s\beta & s\alpha & c\alpha c\beta\end{bmatrix} \tag{8}$$

According to the known conditions, the inverse solution of the 2-UPS/RR mechanism can be obtained as:

$$\begin{cases} l_1=\sqrt{\begin{array}{c}\left(-x_{U_1}+x_{S_1}c\beta+z_{S_1}s\beta\right)^2+\left(-y_{U_1}+x_{S_1}sas\beta+y_{S_1}ca-z_{S_1}sac\beta\right)^2\\ +\left(h-x_{S_1}cas\beta+y_{S_1}sa+z_{S_1}cac\beta\right)^2\end{array}}\\ l_2=\sqrt{\begin{array}{c}\left(-x_{U_2}+x_{S_2}c\beta+z_{S_2}s\beta\right)^2+\left(-y_{U_2}+x_{S_2}sas\beta-y_{S_2}ca-z_{S_2}sac\beta\right)^2\\ +\left(h-x_{S_2}cas\beta-y_{S_2}sa+z_{S_2}cac\beta\right)^2\end{array}}\end{cases} \tag{9}$$

According to Eq. 8, the inverse solution of the mechanism can be obtained when the geometric parameters of the mechanism and the rotation angle of the movable platform around the axis are known.

2.3 Related biomechanical theories

In AMS, inverse kinematics analysis must solve the redundancy problem (not enough equilibrium equations are available to determine all the muscle forces) of the muscle system [12], which involves the problem of muscle recruitment, which is solved by converting the problem of muscle recruitment into a mathematical optimization problem to minimize the objective function G. This is due to the fact that we have more muscles than strictly necessary to drive most motions. The solution for muscle recruitment in inverse dynamics is usually expressed as a mathematical optimization problem, which minimizes the value by the objective function $G\left(f^{(M)}\right)$ [13]:

$$G\left(f^{(M)}\right)=\sum_{i=1}^{n^{(M)}}\left(\frac{f_i^{(M)}}{N_i}\right)^p \tag{10}$$

$$Cf=r \tag{11}$$

$$\left[C^{(M)}C^{(R)}\right]\begin{Bmatrix}f^{(M)}\\ f^{(R)}\end{Bmatrix}=r \tag{12}$$

$$0\le f^{(M)}\le N_i, i\in(1,2\ldots n) \tag{13}$$

where G is the objective function of the mathematical optimization problem, and its solution depends on the maximum value of the unknown force in the problem. In Eq. 10, $f_i^{(M)}$ is the muscle force of the i-th muscle, and the internal force f is divided into two parts, namely muscle force $f^{(M)}$ and joint force $f^{(R)}$. N_i is the muscle strength of the i-th muscle, and $n^{(M)}$ is the number of muscles. Let $p=3$ to ensure the minimum fatigue strength. Equation 11 is the dynamic balance equation, C is the coefficient matrix, and r is used to represent all known force vectors. Equation 13 represents the non-negative constraint on muscle strength, which means that within a certain strength range (0-N_i), the muscle can only be pulled but not pushed.

Existing studies have used a single muscle to characterize the activation dynamics of muscles and the dynamics of tendon contraction. Muscle drive models include models of muscle activation and contraction dynamics, and allow calculation of muscle force, fiber length, and other difficult to measure parameters. Due to the complexity of biological muscles, many simplifications were made when developing the tendon model. It is assumed that the tendon driver is an extensible string that is massless, frictionless, attached to the bones, and other structures. All muscle fibers are assumed to be straight, parallel, coplanar, and of equal length, and simplify the geometry [14]. At the same time, the fiber geometry and height are also assumed to be constant.

Each actuator is modeled as a 3-element HILL-type tendon unit (Fig. 3). Muscles are described by an active contraction element (CE) that generates the active force and a passive parallel elastic element (PEE). The tendon part uses a nonlinear series elastic element (SEE) that can express the mechanical properties of the tendon.

The length of the muscle and tendon elastic unit is:

$$L_{MT}=L_T+L_M\ \cos\alpha \tag{14}$$

Among them, L_T is the length of the tendon unit, L_M is the length of the muscle unit, and α is the pinnate angle.

Muscle force can be expressed as [15]:

$$F_M=F_A+F_P \tag{15}$$

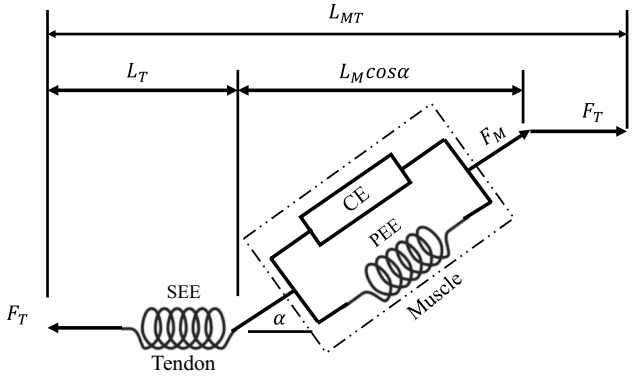

Fig. 3 HILL-type model [3]

Among them, F_A and F_P represent the main force and passive force generated by the muscle under the standardized muscle length (L_N). The normalized active force (F_A) is expressed as a function of the muscle fiber velocity (V^M), muscle fiber length, and the muscle activation (a):

$$F_A = \frac{V^M \cdot b}{V^M_{\max} \cdot (0.25 + 0.75a)} + af \tag{16}$$

$$b = \begin{cases} af + \frac{F_A}{A_f}; F_A \le af \\ \frac{(2+\frac{2}{A_f})(af F^M_{\max} - F_A)}{(F^M_{\max} - 1)}; F_A > af \end{cases} \tag{17}$$

$$f = e^{\frac{-(L_N-1)^2}{\gamma}} \tag{18}$$

$$F_P = \frac{e^{\frac{K_P(L_N-1)}{\varepsilon^m_0}}}{e^{K_p}} \tag{19}$$

The degree of muscle activation ($a_{min} < a < 1$) (Table 1).

Table 1 Naming of related parameters

Parameter	Definition
V^M	The muscle contraction velocity
V^M_{max}	The maximum muscle contraction velocity
A_f	The force–velocity shape factor
F^M_{max}	Maximum muscle strength
γ	Active force–length shape factor
L_N	Normalized muscle fiber length
ε^M_0	The passive muscle strain due to maximum isometric force
K_p	The exponential shape factor

3 Results

3.1 Model analysis

The variable parameters are set through parameter research, and the limits of the variable parameters are constrained. After a series of adjustments, it is finally determined that the relevant rehabilitation parameter values are $\begin{cases} A_i = [0, \alpha] \\ B_i = [0, 0] \end{cases}$ and $\begin{cases} A_k = [pi, \beta] \\ B_k = [pi/2, 0] \end{cases}$. During the movement, the corresponding values of α and β are adjusted for trajectory planning.

The ankle rehabilitation robot drives the ankle joint to perform rehabilitation exercises by driving the platform, simulating the motion state of the ankle joint of a normal person, so that the patient's ankle joint and calf muscles can be comprehensively trained to restore the basic functions of the ankle joint. By analyzing the changes of different muscle parameters and the changing trend of joint force of the man–machine coupling model under different related rehabilitation positions, the effectiveness of muscle participation in the training can be obtained during the rehabilitation process. As during exercise, the calf muscles need to work in coordination and force uniformly, so a reasonable rehabilitation strategy can be formulated through the law of changes in the relative force of the lower limbs. The rehabilitation conditions are obtained from the biomechanical model of the human movement system presented in AnyBody software (Fig. 4). Muscle force is affected by many factors, including muscle length, contraction speed, and load size. Due to the addition of foot pedals in this model, which results in a different force situation during rehabilitation compared to normal walking, corresponding changes in.

In the early stage of rehabilitation, passive rehabilitation (rehabilitation is led by the machine) is mainly performed. During passive rehabilitation, the muscle does not exert force, and the ankle joint is quickly recovered through the set rehabilitation trajectory, which has an excellent effect on the recovery of the ankle joint [16], as the calf muscle group is the main muscle group that drives the ankle joint movement, and not all of them take on a large force during the process of rehabilitation exercise. It can be seen from Fig. 5 that during the rehabilitation process within a cycle, the right leg muscles reach a peak value at 1.0 s, and the muscle recruitment is also large at this moment. Soleus, peroneus brevis, and extensor digitorum longus were selected as the research objects to investigate the changing pattern of biomechanical response of ankle joint under different trajectories according to the force condition of calf muscles.

3.2 Man–machine model verification experiments

The acquisition system used in this paper is the Wave Plus wireless EMG acquisition system released by Cometa srl,

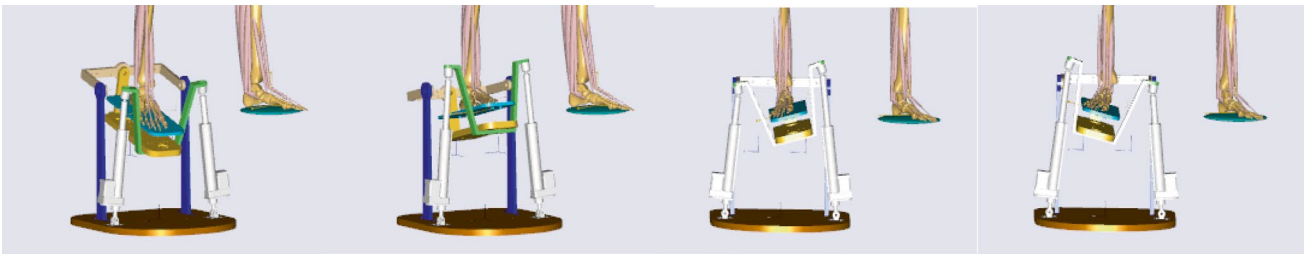

Fig. 4 Biological model of the ankle joint related rehabilitation position

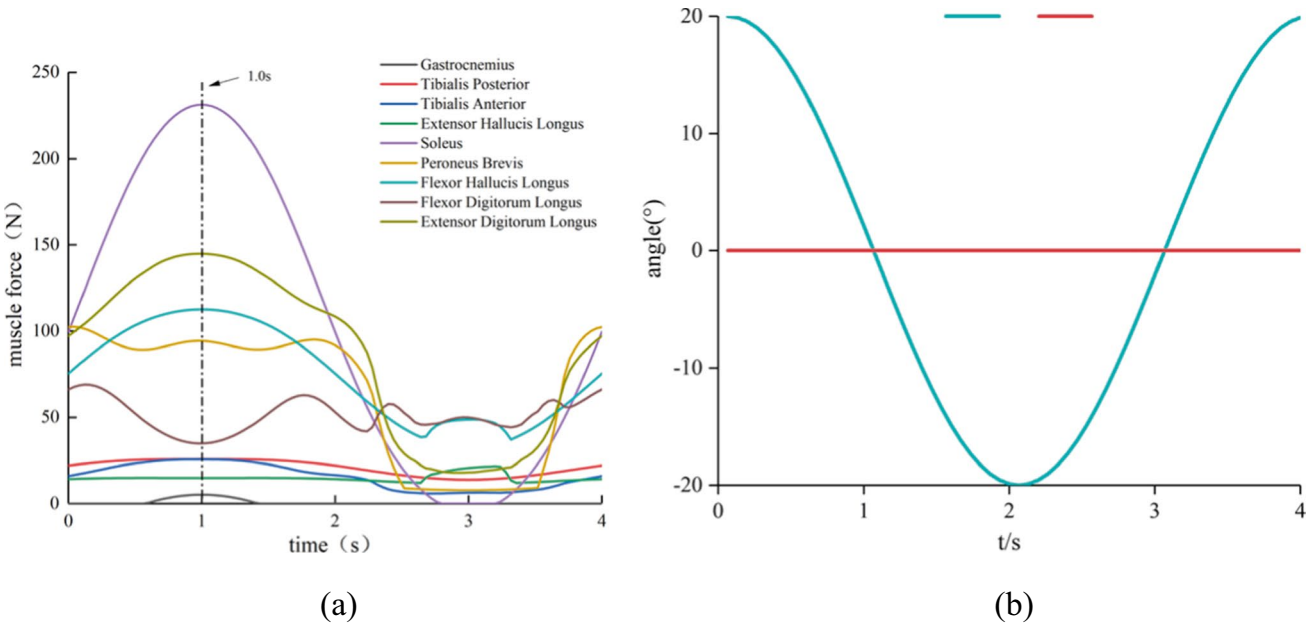

Fig. 5 **A** The force of calf muscles during the rehabilitation. **b** Rehabilitation trajectory during rehabilitation

which is an innovative multi-channel wireless surface EMG system with an accelerometer. The Wave Plus wireless acquisition system mainly includes electrodes (dry or wet), signal receivers, data transmission lines, and wireless electromyography, as shown in Fig. 6.

The Wave Plus wireless EMG acquisition system is a system for biological signal data collection, which can amplify 4 acquisition channels at the same time, and the acquisition frequency is 2000 Hz.

The validated calculation model can be used to predict the biomechanical response under different parameters without the need for expensive experiments. Before using the man–machine coupling model, the simulation output should be compared and analyzed with the processed experimental data to verify the accuracy of the established model. Figure 7 shows volunteers using an ankle joint rehabilitation robot to collect signals under active rehabilitation model (rehabilitation according to the volunteer's exercise intention).

Related studies [17–19] have used the EMG signal MVC calibration experiments to verify the scientific and feasibility of the related model. The defined model is executed with the same rehabilitation motion trajectory when the ankle rehabilitation robot experimental signal is collected, and finally, the muscle activity obtained from the simulation and the experiment is compared and analyzed, as shown in Fig. 8.

Figure 8a shows the comparison of the simulation results of the tibialis anterior, peroneus brevis, gastrocnemius, and soleus muscles with EMG muscle activity under the ankle 20° plantar/dorsiflexion action. The curve trends of the simulation results and the experimental calculation results have good consistency. Figure 8b shows the comparison between the simulation of tibialis anterior and peroneus

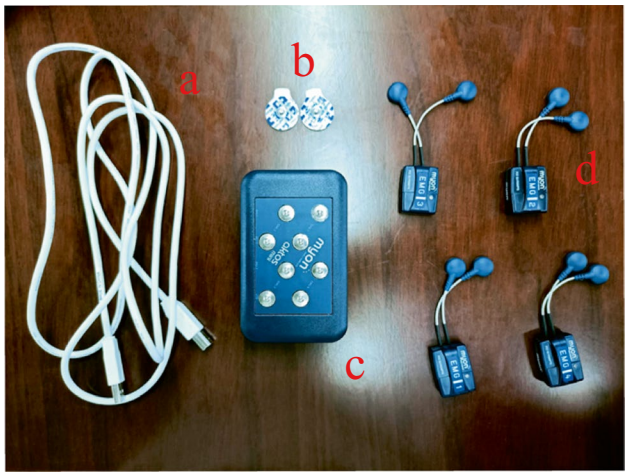

Fig. 6 Wave Plus wireless EMG acquisition system. (**a**) Data transmission line, (**b**) electrode sheet, (**c**) signal receiver, (**d**) signal acquisition unit

brevis muscles under 20° varus/valgus maneuvers with EMG muscle activity. The overall trend changes of the two have good consistency.

3.3 Muscle force analysis of lower limbs

The main forms of movement of the ankle joint are toe flexion, dorsiflexion, varus, valgus, adduction, and abduction. Rehabilitation of the ankle joint requires the human body to be in a normal sitting position, with the feet fixed on the platform, and the calf is naturally straight and relaxed. Under the traction of the mechanism, the calf and ankle muscles can be pulled to achieve a relaxing effect. The movement of the ankle joint has a safe range [20], as shown in Table 2. During the simulation, the angle of the ankle joint must be controlled within a safe range.

The changes in the force of the muscles under different angles of plantar dorsiflexion can be seen from Fig. 9. Figure 9a shows the effect of the angle of plantar dorsiflexion on the muscle force of the soleus. In the first half of the cycle, the muscle force of the soleus first increases and then decreases, reaching the maximum and minimum values at 1.0 s and 3.0 s, respectively. Since the soleus muscle plays a major role in plantar flexion, it reaches the peak of muscle force at the maximum plantar flexion in 1 s, and as the angle of plantar flexion increases, the peak value of the curve also increases. The maximum peak muscle force is 250 N. In the second half of the cycle, rehabilitation gradually transitions from plantar flexion to dorsiflexion, and the changes in muscle force also show a trend of first decreasing and then increasing. From Fig. 9b, it can be seen that the muscle force changes of the peroneus brevis in the first half of the cycle are relatively smooth, floating up and down between 90 and 110 N, and the muscle force of the second half of the cycle shows a trend of first decreasing and then increasing, reaching the minimum value at 3.0 s. With the increase of the angle of plantar dorsiflexion, the muscle force around 3.0 s basically does not change, and the muscle force when reaching 20° dorsiflexion is only 10 N. Figure 9c shows the effect of the angle of plantar dorsiflexion on the muscle force of the extensor digitorum longus. In the first half of the rehabilitation cycle, the curve first increases and then decreases. And as the angle of plantar dorsiflexion increases, the range of muscle force changes gradually, varying between 100 and 140 N. When rehabilitation transitions from plantar flexion to dorsiflexion, the curve becomes a change that is first decreasing and then increasing. Through the comparative analysis of the above curves, it can be inferred that different muscles have different sensitivities to changes in the rehabilitation angle. Therefore, during rehabilitation, the trajectory must be reasonably planned according to the muscles to be restored to shorten the rehabilitation training time. When we perform early passive rehabilitation, we can determine the plantar dorsiflexion angle according to the patient's different rehabilitation periods and the patient's muscle rehabilitation.

3.4 Joint force analysis

The human ankle joint is composed of the articular surface of the tibia and the lower end of the fibula and the talus pulley. It is one of the most complex joints in the human bones and plays an important role in the body's standing and maintaining balance [21]. The rehabilitation of joints is also crucial in the rehabilitation process. Through the inverse kinematics analysis module, simulation analysis is carried out under three different rehabilitation trajectories, and the changes of joint force in one cycle are obtained. The ankle reaction force mainly includes the component forces in three directions (F_x, F_y, F_z). The total joint reaction force can be obtained by Formula (20).

$$F_t = \sqrt{F_x{}^2 + F_y{}^2 + F_z{}^2} \tag{20}$$

Figure 10 shows the influence of different rehabilitation trajectories on joint force. In the first half of the rehabilitation cycle, the joint force shows a pattern of change first and then decreases, with the maximum peak value of 865 N. In the second half of the cycle, the curve changes to a trend of first decreasing and then increasing, and the joint force is more sensitive to the dorsiflexion. Figure 10b is a variation of the angle of varus effect on joint force curve which shows that the change varus angle for the joint force impact is not great. The curve shows a cyclical change rule, the joint force changes in a state of valgus is relatively smooth, only about 100 N, it can be inferred that the effect of varus on the ankle joint rehabilitation is not very obvious. Compared

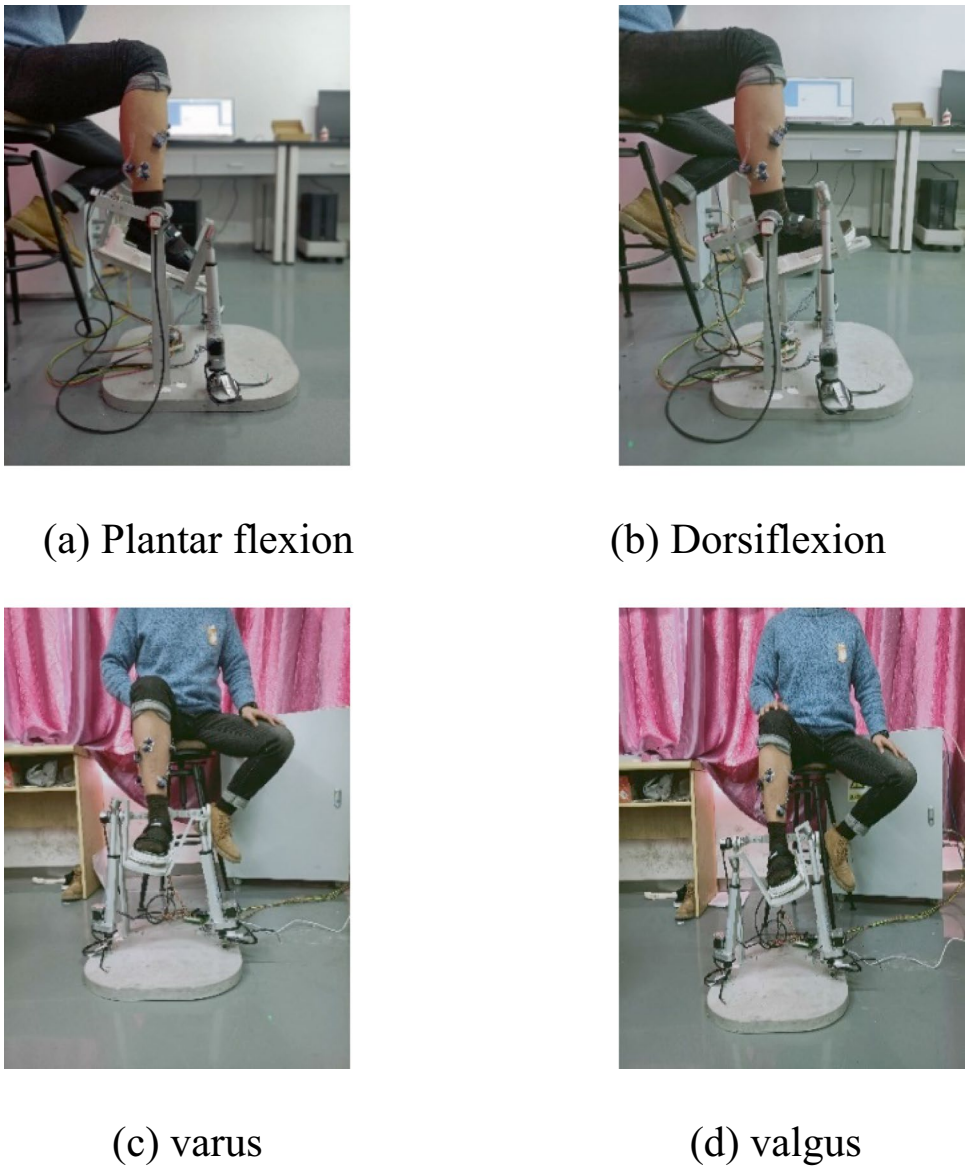

Fig. 7 Ankle rehabilitation robot signal acquisition

with varus, when the rehabilitation is in a state of valgus, the joint force presents an increasing trend, and the magnitude of the change decreases. Figure 10c shows the effect of the change of the compound motion angle on the joint force, and the overall trend is the same as the change of plantar dorsiflexion. The peak joint force appears later than the plantar dorsiflexion.

Figure 11 is a comparative analysis of the joint force of the three rehabilitation trajectories at a rehabilitation angle of 15°. It can be seen from the figure that within one exercise cycle, the curve change trend of plantar dorsiflexion and compound exercise is roughly the same, while the change of varus was relatively stable, floating between 600 and 700 N. The correlation analysis of the three rehabilitation trajectories showed that the correlation coefficient between plantar dorsiflexion and compound exercise reached 0.99 ($P<0.05$). It shows that the change of compound motion is mainly dominated by plantar dorsiflexion, but it is also affected by inversion and eversion, making the curve between the two. It can be shown that compound exercises can achieve the effects of plantar dorsiflexion and varus, and the expected rehabilitation requirements and effects can be achieved by adjusting the angles of the two.

In the process of ankle rehabilitation, it is necessary to avoid improper rehabilitation resulting in poor rehabilitation and secondary muscle injure. Due to the different strengths of each muscle, therefore, the muscle activation degree is used to characterize the force characteristics of the lower extremity muscles in the rehabilitation process. The muscle activation degree is calculated by Formula (21), regardless of the strength difference

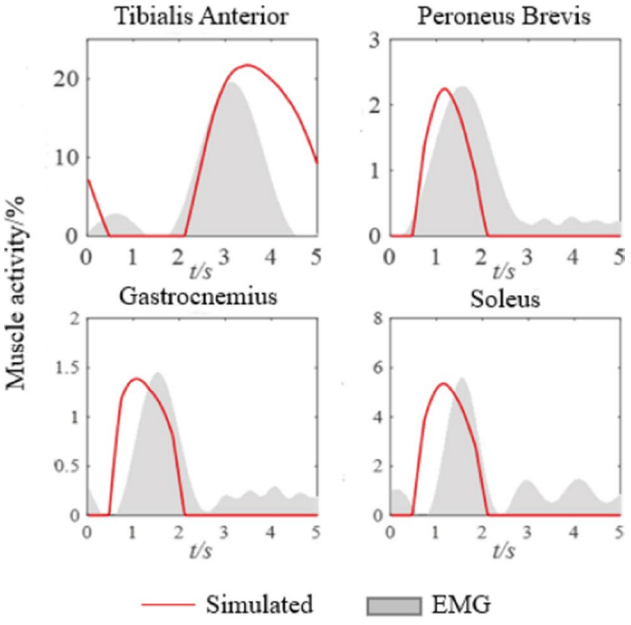

(a) 20 ° plantar / dorsiflexion

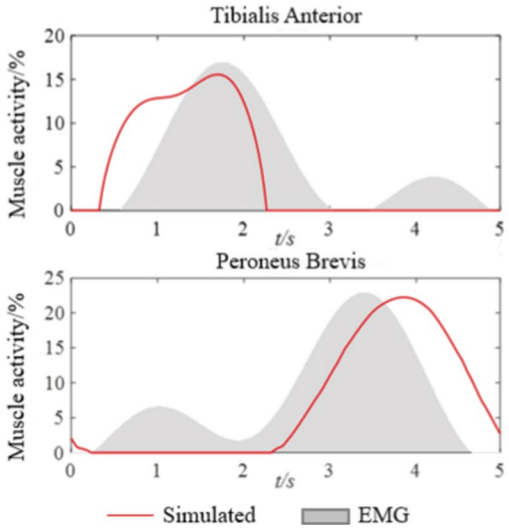

(b) 20 ° varus / valgus

Fig. 8 Computed muscle activations compared to measured EMG for the major calf muscle during plantar/dorsiflexion and varus/valgus. Simulated muscle activity in **a** 20° plantar/dorsiflexion for tibialis anterior, peroneus brevis, gastrocnemius, and soleus and **b** 20° varus/valgus for tibialis anterior and peroneus brevis is shown in red. The corresponding experimental EMG signals are shown by the gray shaded regions

between muscles. Figure 9 shows the changes in maximum muscle activation under different rehabilitation angles.

Table 2 Ankle joint motion angle range

Exercise	Range of motion angle(°)
Plantar flexion	0–35
Dorsiflexion	0–25
Varus	0–30
Valgus	0–25
Adduction	0–20
Outreach	0–20

$$Act = \frac{F}{F\ \max} \times 100\% \tag{21}$$

Among them, *Act* is the degree of muscle activation, which can be understood as the proportion of the current muscle output during the rehabilitation process that is equivalent to its maximum muscle output, *F* is the current muscle strength, and *F* max is the muscle produced when the muscle is in the maximum force state.

According to Fig. 12, it can be seen that when using this ankle rehabilitation robot for rehabilitation, as the rehabilitation angle increases, the maximum muscle activation during varus and valgus is in a steadily rising state, but the degree of change is not large, within 10%. However, the degree of muscle activation of plantar dorsiflexion varies greatly. The rehabilitation angle is from 5° to 20°, and the degree of muscle activation is increased by as much as 23%. However, during the rehabilitation, all muscle activation degrees did not exceed 60%, and no secondary injure to the muscles would be caused. This also verifies that the rehabilitation robot mainly relies on the movement in the direction of plantar dorsiflexion during rehabilitation. By adjusting the movement in the direction of plantar dorsiflexion, the rehabilitation is supplemented by inversion and valgus, which can meet some basic rehabilitation requirements.

4 Discussion

Physical therapy is indispensable in the process of ankle rehabilitation. In the course of treatment, patients can restore a limited range of motion and weak muscles, achieve dynamic balance, and then recover motor function gradually [22]. Therefore, it is a long-term and intensive process. However, in traditional physical therapy process, the patient's ankle joint is manually moved by the doctor to restore basic ankle joint movement, which requires the doctor to have long-term training experience and patience [23]. As a result, robot-assisted therapy is a better choice. Nowadays, with the rapid development of virtual reality technology, it has been widely used in rehabilitation robots.

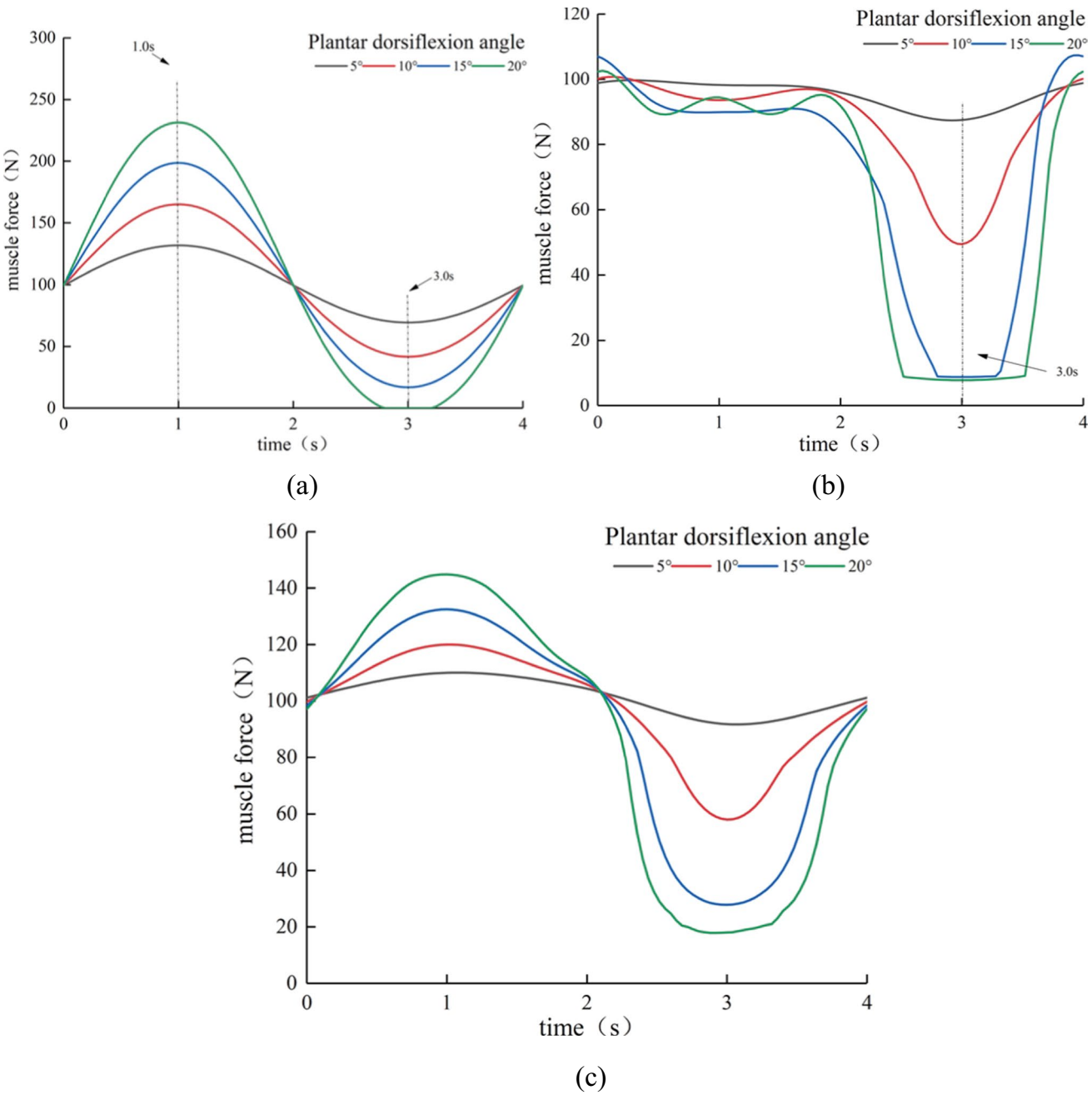

Fig. 9 The muscle force of the three muscles during rehabilitation: **a** soleus, **b** peroneal brevis, **c** extensor digitorum longus

A 2-UPS/RR parallel robot has the advantages of lower secondary damage and easy operability, based on the biomechanics simulation results, the workspace of the ankle rehabilitation robot and its influence on the muscle force and joint force of the lower limbs. Compared with previous studies, the 2-UPS/RR robot has a larger space and better coordination for lower limb rehabilitation by biomechanics analysis [24–26]. The previous studies mainly focus on the relationship between rehabilitation robot and institutional configuration. Wang C [24] proposed that mechanism can actualize the rotational movements of the ankle in three directions while at the same time the mechanism center of rotations can match the ankle axes of rotations. Ahmetcan Erdogan [25] invented a reconfigurable ankle exoskeleton with series elastic actuation which can cover the whole range of motion of the human ankle, and in the another parallel mechanism that can support the ground reaction forces/torques transferred to the ankle. Leiyu Zhang [26] proposed a

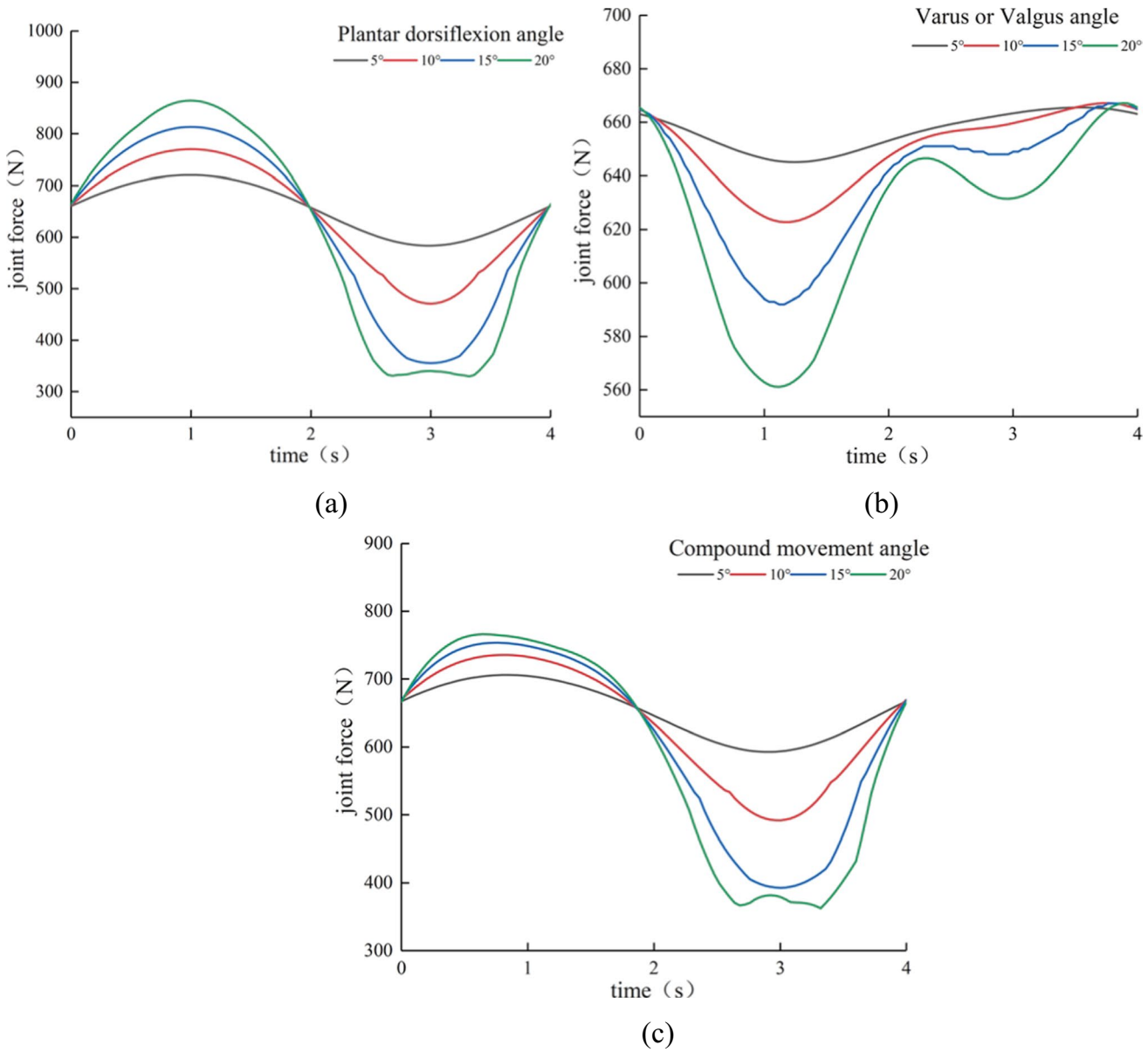

Fig. 10 The joint force of different rehabilitation trajectories. **a** Plantar dorsiflexion, **b** varus or valgus, **c** compound movement

parallel ankle rehabilitation robot; this robot can well meet the needs of ankle rehabilitation and the scope of ankle rehabilitation.

By analyzing the influence of plantar dorsiflexion on the related muscles and the changing trend of joint force under the three kinds of rehabilitation trajectory, it was concluded that the biological response of muscles to different rehabilitation trajectories changes, so the ankle joint rehabilitation must be targeted. On the basis of biomechanical simulation, by considering muscle force and joint force, and comparing study of different rehabilitation trajectories and rehabilitation angles comprehensively, it can be found that in the state of plantar flexion, the muscle force of lower limbs and the joint force of ankle joint were both high. On the contrary, in the dorsiflexion state, the change trend was also completely opposite to that in the dorsiflexion state, and the difference between the peak value and valley value reached 550 N. Moreover, with increase of the plantar dorsiflexion angle, the peak value and valley value appeared at the same time point, and the change trend of the curve was roughly the same, indicating that the ankle rehabilitation robot had a periodic rehabilitation law. In addition, when performing rehabilitation on the sagittal plane of the ankle joint, the angle during the plantar flexion process should be controlled so that the muscle force that the muscles can withstand did not exceed the threshold.

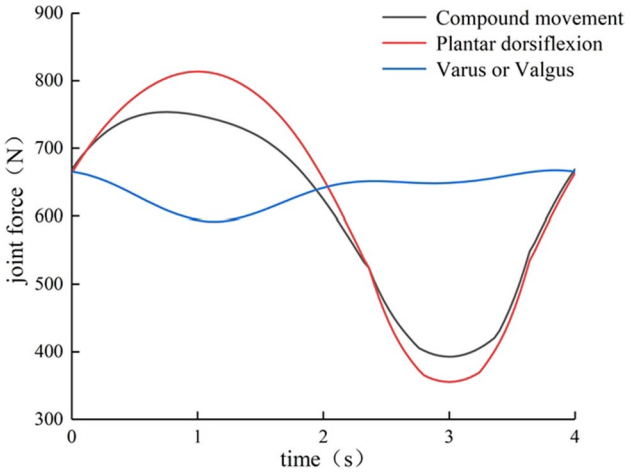

Fig. 11 The joint force of each rehabilitation trajectory when the angle was 15°

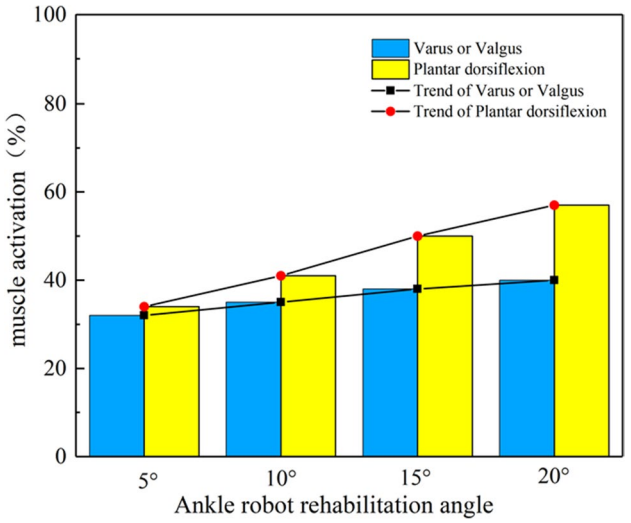

Fig. 12 Comparison of maximum muscle activation under different rehabilitation angles

The correlation coefficient between plantar dorsiflexion and compound motion reached 0.99, indicating that joint motion under compound motion was mainly affected by plantar dorsiflexion. In the first half of the cycle, varus and valgus can reduce joint force while in the second half of the cycle, varus and valgus can increase joint force, and the rehabilitation angle of compound sports can be adjusted by adjusting the angle of varus and valgus. During the rehabilitation process, the maximum muscle activation did not exceed 60% for avoiding secondary muscle injure. When performing rehabilitation exercises in the early stage of rehabilitation, the physician should combine the patient's own condition and related rehabilitation effects to gradually increase the rehabilitation angle. At the same time, the patient must choose the corresponding rehabilitation trajectory and perform targeted rehabilitation exercises to strengthen muscles.

Compared with the rehabilitation analysis of other ankle rehabilitation robots, it has formed a systematic evaluation process. Through modeling and analysis of different rehabilitation trajectories and rehabilitation angles, the changes of muscle force and joint force of related muscles were obtained, and the changes of parameters were considered for both. The impact of secondary injuries in the rehabilitation process, to a certain extent, has been avoided, with comprehensive consideration of the rehabilitation effect in the process of lower limb rehabilitation and corresponding recommendations for early rehabilitation and rehabilitation strategies.

5 Conclusion

For the current research on ankle joint rehabilitation robots, most of them focus on mechanism design, and lack of research on the biomechanical response of lower limb muscles. Using the designed 2-UPS/RR parallel ankle joint rehabilitation robot, the man–machine coupling model is established through AMS and the rehabilitation is analyzed. The influence of the parameters on the muscle force and joint force of the lower limbs and the following results are obtained.

(1) The designed 2-UPS/RR ankle joint rehabilitation robot is analyzed by inverse solution. According to closed-loop vector method, the inverse kinematics solution of the link length is obtained. When the structure parameters and mechanism are known, the rotation angle of the shaft can get the displacement of each push rod. Thus, the mechanism can meet the basic requirements of ankle joint rehabilitation.
(2) Through the inverse kinematics analysis module of AMS, the variation rule of main leg muscles with metatarsal dorsal flexion angle is revealed. The simulation results show that different muscles have different sensitivities to the change of rehabilitation angle. During rehabilitation, the rehabilitation trajectory must be planned according to actual conditions.
(3) The mechanical model of the ankle joint was established and the variation laws of the ankle joint force under the three rehabilitation trajectories were compared and analyzed. Through the comparison and correlation analysis of the joint force, it can be shown that the composite movement can achieve the effects of metatarsal dorsal flexion and valgus at the same time, and the angle of both can be adjusted to achieve the desired rehabilitation effect.

The analysis results show that the human–machine coupling model of 2-UPS/RR ankle rehabilitation robot has potential use in formulating rehabilitation strategies and planning rehabilitation trajectory, which contribute to rehabilitation and treatment of joint diseases, and provide more reasonable suggestions for early rehabilitation.

Supplementary information The online version contains supplementary material available at https://doi.org/10.1007/s11517-022-02704-y.

Funding The authors would like to thank the financial support from the National Natural Science Foundation of China (grant no. 61801122).

Declarations

Ethical approval and consent to participate For this type of study, formal consent is not required. The study was conducted according to the guidelines of the Declaration of Helsinki, and approved by the institutional review board of the School of Mechanical Engineering and Automation of Fuzhou University (202108

Conflict of interest The authors declare no competing interests.

References

1. Van Houcke J, Schouten A, Steenackers G et al (2017) Computer-based estimation of the hip joint reaction force and hip flexion angle in three different sitting configurations[J]. Appl Ergon 63:99–105
2. Hazrati E, Azghani MR (2018) The effect of saddle height and saddle position changes from pedal on muscles and joints behaviors in ergometer: a parametric study[J]. Proc Inst Mech Eng [H] 232(12):1219–1229
3. Rajagopal A, Dembia C, Demers MS et al (2016) Full-body musculoskeletal model for muscle-driven simulation of human gait[J]. IEEE Trans Biomed Eng 63(10):2068–2079
4. Hamner SR, Seth A, Delp SL (2010) Muscle contributions to propulsion and support during running[J]. J Biomech 43(14):2709–2716
5. Zongxing L, Xiangwen W, Shengxian Y (2020) The effect of sitting position changes from pedaling rehabilitation on muscle activity[J]. Computer Methods in Biomechanics and Biomedical Engineering, 1–10
6. Fenfang Z, Zhu G, Tsoi Y H, et al (2014) A computational biomechanical model of the human ankle for development of an ankle rehabilitation robot[C]//2014 IEEE/ASME 10th International Conference on Mechatronic and Embedded Systems and Applications (MESA). IEEE, 1–6
7. Shi M, Yang C, Zhang D (2021) A novel human-machine collaboration model of an ankle joint rehabilitation robot driven by EEG signals[J]. Mathematical Problems in Engineering, 2021
8. Wang Y, Mei Z, Xu J, et al (2012) Kinematic design of a parallel ankle rehabilitation robot for sprained ankle physiotherapy[J]. Advanced ence Letters 1643 - 1649
9. Dai JS, Zhao T, Nester C (2004) Sprained ankle physiotherapy based mechanism synthesis and stiffness analysis of a robotic rehabilitation device[J]. Auton Robot 16(2):207–218
10. Jamwal PK, Xie SQ, Tsoi YH et al (2010) Forward kinematics modelling of a parallel ankle rehabilitation robot using modified fuzzy inference[J]. Mech Mach Theory 45(11):1537–1554
11. Saglia JA, Tsagarakis NG, Dai JS et al (2009) A high-performance redundantly actuated parallel mechanism for ankle rehabilitation[J]. Int J Robot Res 28(9):1216–1227
12. Pai DK (2010) Muscle mass in musculoskeletal models[J]. J Biomech 43(11):2093–2098
13. Adam Siemienski (1989) Soft saturation, an idea for load sharing between muscles. Application to the study of human locomotion[C]// Biolocomotion: A Century of Research Using Moving Pictures
14. Zajac FE (1989) Muscle and tendon: properties, models, scaling, and application to biomechanics and motor control[J]. Crit Rev Biomed Eng 17(4):359–411
15. Sartori M, Reggiani M, Lloyd DG, et al (2011) A neuromusculoskeletal model of the human lower limb: towards EMG-driven actuation of multiple joints in powered orthoses[C]// IEEE International Conference on Rehabilitation Robotics. Beijing,China IEEE
16. Terada M, Pietrosimone BG, Gribble PA (2013) Therapeutic interventions for increasing ankle dorsiflexion after ankle sprain: a systematic review[J]. J Athletic Train 48(5):696–709
17. Pontonnier C, De Zee M, Samani A et al (2014) Strengths and limitations of a musculoskeletal model for an analysis of simulated meat cutting tasks [J]. Appl Ergon 45(3):592–600
18. Dupré T, Dietzsch M, Komnik I et al (2019) Agreement of measured and calculated muscle activity during highly dynamic movements modelled with a spherical knee joint [J]. J Biomech 84:3–80
19. Dubowsky SR, Rasmussen J, Sisto SA et al (2008) Validation of a musculoskeletal model of wheelchair propulsion and its application to minimizing shoulder joint forces [J]. J Biomech 41(14):2981–2988
20. Yao L G, Liao Z W, Lu Z X, et al (2018) Nutation motion based trajectory planning for a novel hybrid ankle rehabilitation device[J]. J Mech Eng (online publishing), 1–8
21. Zhang M, Claire Davies T (2013) Effectiveness of robot-assisted therapy on ankle rehabilitation – a systematic review[J]. J Neuro Eng Rehabilitation 10(1):30–38
22. Li J, Zhang Z, Tao C et al (2017) A number synthesis method of the self-adapting upper-limb rehabilitation exoskeletons[J]. Int J Adv Rob Syst 14(3):1729881417710796
23. Zhou Z, Zhou Y, Wang N, et al (2014) On the design of a robot-assisted rehabilitation system for ankle joint with contracture and/or spasticity based on proprioceptive neuromuscular facilitation[C]// 2014 IEEE International Conference on Robotics and Automation (ICRA 2014), Hong Kong, China 31 May -7 June 2014
24. Wang C, Fang Y, Guo S et al (2013) Design and kinematical performance analysis of a 3-RUS/R RR redundantly actuated parallel mechanism for ankle rehabilitation[J]. J Mech Robot 5(4):041003
25. Erdogan A, Celebi B, Satici AC et al (2017) Assist on-ankle: a reconfigurable ankle exoskeleton with series-elastic actuation[J]. Auton Robot 41(3):743–758
26. Zhang L, Li J, Dong M, et al (2019) Design and workspace analysis of a parallel ankle rehabilitation robot (PARR)[J]. Journal of healthcare engineering, 2019

Publisher's note Springer Nature remains neutral with regard to jurisdictional claims in published maps and institutional affiliations.

Springer Nature or its licensor (e.g. a society or other partner) holds exclusive rights to this article under a publishing agreement with the author(s) or other rightsholder(s); author self-archiving of the accepted manuscript version of this article is solely governed by the terms of such publishing agreement and applicable law.

You Shengxian received the B.S. degree from Fujian Agriculture and Forestry University in mechanical engineering and automation in 2015. Now, he is a postgraduate student in the School of Mechanical Engineering and Automation, Fuzhou University. He has engaged in the research of the lower limb rehabilitation robot and human biomechanics. His research interests include establishment of human–machine coupling model, inverse kinematics analysis, and application of lower limb rehabilitation machine.

Lu Zongxing is an Associate Professor at the School of Mechanical Engineering and Automation at Fuzhou University. He has received the Ph.D. degree at the School of Mechanical Engineering, Beijing Institute of Technology, in 2016. He received his bachelor degree from Beijing Institute of Technology in 2010. His research mainly includes dual-robot cooperate system, the development of lower limb rehabilitation robot system, electromechanical control, and evaluation of ultrasound muscle characteristics.

Wang Jing received her B.S. degree from Fuzhou University in mechanical engineering and automation in 2015. She is currently working towards the M.S. degree in the School of Mechanical Engineering and Automation, Fuzhou University. Her research interest includes motion recognition based on sEMG signal.

Guo Lin received his B.S. degree from Fuzhou University in mechanical engineering and automation in 2015. He is currently working towards the M.S. degree in the School of Mechanical Engineering and Automation, Fuzhou University. His research interest includes motion recognition based on ultrasound signal.